

Lattice Boltzmann models for the simulation of flows through microchannels

Victor E. Ambruş^{1,2} and Victor Sofonea¹

¹ Centre for Fundamental and Advanced Technical Research, Romanian Academy
Bd. Mihai Viteazul 24, RO 300223 Timișoara, Romania

² Department of Physics, West University of Timișoara
Bd. Vasile Parvan 4, RO 300223 Timișoara, Romania



12/01/2016



- 1 The Boltzmann equation
 - The Boltzmann distribution function
 - Diffuse reflection
- 2 Quadrature-based lattice Boltzmann models
 - Full-range Gauss-Hermite (HLB) models
 - Half-range Gauss-Hermite (HHLB) models
- 3 Numerical results
 - Couette flow
 - Poiseuille flow
- 4 Conclusion

The lattice Boltzmann method

- The lattice Boltzmann method provides a simple algorithm to obtain approximate solutions of the Boltzmann equation.
- At small Knudsen number $Kn = \lambda/L$, the Navier-Stokes(-Fourier) regime can be recovered.
- At high Kn , beyond Navier-Stokes effects (slip velocity, temperature jump, etc.) can be recovered, allowing the simulation of flows through microchannels, rarefied flows, etc.
- Multiphase and multicomponent flows are easily implemented (interface tracking not required): glassy fluids, foams, phase separation, droplets dynamics, etc.

The Boltzmann equation

- In the BGK approximation for the collision term, the Boltzmann equation reads:

$$\partial_t f + \frac{1}{m} \mathbf{p} \cdot \nabla f + \mathbf{F} \cdot \nabla_{\mathbf{p}} f = -\frac{1}{\tau} (f - f^{(\text{eq})}),$$

where $f \equiv f(\mathbf{x}, \mathbf{p}, t)$ is the one-particle distribution function, $\tau \sim \mathbf{K}n/n$ is the relaxation time and $f^{(\text{eq})}$ is the Maxwell-Boltzmann equilibrium distribution (D is the number of space dimensions):

$$f^{(\text{eq})}(n, \mathbf{u}, T) = \frac{n}{(2\pi m K_B T)^{\frac{D}{2}}} \exp \left[-\frac{(\mathbf{p} - m\mathbf{u})^2}{2m K_B T} \right].$$

Moments of f

- Macroscopic properties given as moments of order N of f :

$$N=0: \quad \text{number density:} \quad n = \int d^D p f,$$

$$N=1: \quad \text{velocity:} \quad \mathbf{u} = \frac{1}{nm} \int d^D p f \mathbf{p},$$

$$N=2: \quad \text{temperature:} \quad T = \frac{2}{Dn} \int d^D p f \frac{\xi^2}{2m}, \quad (\xi = \mathbf{p} - m\mathbf{u}),$$

$$\text{viscous tensor:} \quad \sigma_{\alpha\beta} = \int d^D p \frac{\xi_\alpha \xi_\beta}{m} f - nT\delta_{\alpha\beta},$$

$$N=3: \quad \text{heat flux:} \quad \mathbf{q} = \int d^D p f \frac{\xi^2}{2m} \frac{\xi}{m}.$$

Transport equations

- The transport equations are obtained by multiplying the Boltzmann equation by $\psi = \{1, \mathbf{p}, \mathbf{p}^2/2m\}$ and integrating over \mathbf{p} :

$$\begin{aligned}\partial_t n + \partial_\alpha(\rho u_\alpha) &= 0, \\ \partial_t(\rho u_\alpha) + \partial_\beta(\rho u_\alpha u_\beta + nT\delta_{\alpha\beta} + \sigma_{\alpha\beta}) &= nF_\alpha, \\ (\partial_t + \partial_\alpha u_\alpha) \left(\frac{3}{2}nT + \frac{\rho \mathbf{u}^2}{2} \right) + \partial_\alpha q_\alpha + \partial_\alpha \left[u_\beta (nT\delta_{\alpha\beta} + \sigma_{\alpha\beta}) \right] &= nu_\alpha F_\alpha.\end{aligned}$$

- Using the Chapman-Enskog expansion:

$$f = f^{(\text{eq})} + f^{(1)}\text{Kn} + f^{(2)}\text{Kn}^2 + \dots, \quad \partial_t = \partial_{t_0} + \text{Kn}\partial_{t_1} + \dots,$$

- the Navier-Stokes limit is recovered at $O(\text{Kn})$:

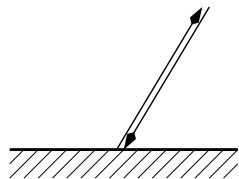
$$\sigma_{\alpha\beta}^{(1)} = -\tau nT \left[\partial_\alpha u_\beta + \partial_\beta u_\alpha - \frac{2}{D} \partial_\gamma u_\gamma \right], \quad q_\alpha^{(1)} = -\frac{D+2}{2m} \tau nT \partial_\alpha T.$$

S. Harris, *An Introduction to the Theory of the Boltzmann Equation* (Holt, Rinehart and Winston, Inc., USA, 1971)

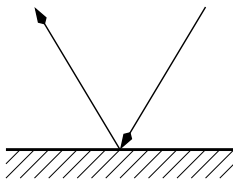
V. E. Ambruş, V. Sofonea, *Phys. Rev. E* **86** (2012) 016708.

Boundary conditions for the distribution function

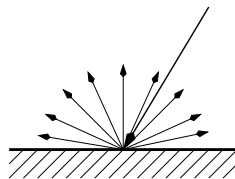
Due to the particle – wall interaction, reflected particles carry some information that belongs to the wall.



bounce back



specular reflection



diffuse reflection

Diffuse reflection: the distribution of *reflected* particles is identical to the Maxwellian distribution function

$$f^{(\text{eq})}(\mathbf{u}_{\text{wall}}, T_{\text{wall}})$$

Microfluidics: $\text{Kn} = \lambda/L$ is non-negligible

⇒ velocity slip u_{slip}

⇒ temperature jump T_{jump}

Diffuse reflection boundary conditions

- The diffuse reflection boundary conditions require:

$$f(\mathbf{x}_w, \mathbf{p}, t) = f^{(\text{eq})}(n_w, \mathbf{u}_w, T_w) \quad (\mathbf{p} \cdot \boldsymbol{\chi} < 0),$$

where $\boldsymbol{\chi}$ is the outwards-directed normal to the boundary.

- Requiring zero mass-flux through the boundary:

$$\int_{\mathbf{p} \cdot \boldsymbol{\chi} > 0} d^3 p f(\mathbf{p} \cdot \boldsymbol{\chi}) + \int_{\mathbf{p} \cdot \boldsymbol{\chi} < 0} d^3 p f^{(\text{eq})}(n_w, \mathbf{u}_w, T_w) (\mathbf{p} \cdot \boldsymbol{\chi}) = 0$$

fixes the density n_w on the wall:

$$n_w = - \frac{\int_{\mathbf{p} \cdot \boldsymbol{\chi} > 0} d^3 p f(\mathbf{p} \cdot \boldsymbol{\chi})}{\int_{\mathbf{p} \cdot \boldsymbol{\chi} < 0} \frac{d^D p}{(2\pi m T_w)^{D/2}} \exp\left[-\frac{(\mathbf{p} - m\mathbf{u}_w)^2}{2mT_w}\right]}.$$

- Diffuse reflection requires the computation of integrals of f and $f^{(\text{eq})}$ over half of the momentum space.

Discretising the momentum space

- In lattice Boltzmann, the velocity space is replaced by a set of discrete velocities \mathbf{p}_k .
- The corresponding distribution function f is replaced by f_k .
- $f^{(\text{eq})}$ in the collision operator is constructed such that the continuum space moments

$$\mathcal{M}_{n_x, n_y, \dots} = \int d^D p f^{(\text{eq})} p_x^{n_x} p_y^{n_y} \dots$$

equal those of the discretised set $\{f_k^{(\text{eq})}\}$:

$$\widetilde{\mathcal{M}}_{n_x, n_y, \dots} = \sum_k f_k^{(\text{eq})} p_{k,x}^{n_x} p_{k,y}^{n_y} \dots$$

such that

$$\widetilde{\mathcal{M}}_{n_x, n_y, \dots} = \mathcal{M}_{n_x, n_y, \dots}.$$

Full-range Gauss-Hermite lattice Boltzmann models

- $f^{(\text{eq})}$ can be factorised as:

$$f^{(\text{eq})} = n g_x g_y \dots, \quad g_\alpha = \frac{1}{\sqrt{2\pi mT}} \exp\left[-\frac{(p_\alpha - mu_\alpha)^2}{2mT}\right].$$

- The moments $\mathcal{M}_{n_x, n_y, \dots}$ can also be factorised:

$$\mathcal{M}_{n_x, n_y, \dots} = \mathcal{M}_{x, n_x} \mathcal{M}_{y, n_y} \dots, \quad \mathcal{M}_{\alpha, n_\alpha} = \int_{-\infty}^{\infty} dp_\alpha g(p_\alpha) p_\alpha^{n_\alpha}.$$

- For N^{th} order accuracy, g_α can be expanded with respect to the full-range Hermite polynomials $H_\ell(p)$:

$$g_\alpha = \frac{e^{-p_\alpha^2/2}}{\sqrt{2\pi}} \sum_{\ell=0}^N \mathcal{G}_\ell H_\ell(p_\alpha), \quad \mathcal{G}_{\alpha, \ell} = \sum_{s=0}^{\ell} \frac{\ell!}{s!(\ell-2s)!} \frac{1}{2^s} \left(\frac{mu_\alpha}{p_{0, \alpha}}\right)^{\ell-2s} \left(\frac{mT}{p_{0, \alpha}^2} - 1\right)^s.$$

- $\mathcal{M}_{\alpha, n_\alpha}$ can be recovered using **HLB(Q_α)**, i.e. the Gauss-Hermite quadrature of order Q_α :

$$\widetilde{\mathcal{M}}_{\alpha, n_\alpha} = \sum_{k=1}^{Q_\alpha} g_{\alpha, k} p_{\alpha, k}^{n_\alpha},$$

where $p_{\alpha, k}$ are the Q_α roots of H_{Q_α} and

$$g_{\alpha, k} = \frac{w_k \sqrt{2\pi}}{e^{-p_{\alpha, k}^2/2}} g_\alpha(p_{\alpha, k}), \quad w_k = \frac{Q_\alpha!}{[H_{Q_\alpha+1}(p_{\alpha, k})]^2}.$$

Full-range Gauss-Hermite lattice Boltzmann models

- M_{α,n_α} can be split corresponding to the + and - p_α semi-axes:

$$M_{\alpha,n_\alpha} = M_{\alpha,n_\alpha}^+ + M_{\alpha,n_\alpha}^-, \quad M_{\alpha,n_\alpha}^+ = \int_0^\infty dp_\alpha g_\alpha p_\alpha^{n_\alpha}, \quad M_{\alpha,n_\alpha}^- = \int_{-\infty}^0 dp_\alpha g_\alpha p_\alpha^{n_\alpha}.$$

- g_α can be expanded in terms of the half-range Hermite polynomials h_ℓ as:

$$g_\alpha = \frac{e^{-p_\alpha^2/2}}{\sqrt{2\pi}} \sum_{\ell=0}^{N_\alpha} h_\ell(|p_\alpha|) \left\{ \frac{1}{2} \sum_{s=0}^{\ell} h_{\ell,s} \left(\frac{mT}{2p_{0,\alpha}^2} \right)^{s/2} \left[(1 + \operatorname{erf} \zeta_\alpha) P_s^+(\zeta_\alpha) + \frac{2}{\sqrt{\pi}} e^{-\zeta_\alpha^2} P_s^*(\zeta_\alpha) \right] \right\},$$

where σ_α is the sign of p_α and P_s^+ and P_s^* are polynomials in $\zeta_\alpha = \sigma_\alpha u_\alpha \sqrt{m/2T}^\dagger$.

- M_{α,s_α}^\pm can be recovered using **HHLB**(Q_α), i.e. the half-range Gauss-Hermite quadrature of order Q_α :

$$\widetilde{M}_{\alpha,s_\alpha}^+ = \int_0^\infty dp_\alpha g_\alpha p_\alpha^{s_\alpha} \simeq \sum_{k=1}^{Q_\alpha} g_{\alpha,k} p_{\alpha,k}^{s_\alpha}, \quad \widetilde{M}_{\alpha,s_\alpha}^- = \int_{-\infty}^0 dp_\alpha g_\alpha p_\alpha^{s_\alpha} \simeq \sum_{k=Q_\alpha+1}^{2Q_\alpha} g_{\alpha,k} p_{\alpha,k}^{s_\alpha},$$

- The quadrature points $p_{\alpha,k}$ are related to the roots r_k of $h_{Q_\alpha}(x)$ through:

$$p_{\alpha,k} = \begin{cases} r_k & 1 \leq k \leq Q_\alpha, \\ -r_k & Q_\alpha < k \leq 2Q_\alpha. \end{cases}$$

- $g_{\alpha,k}$ are defined in terms of the half-range Gauss-Hermite quadrature weights w_k^\ddagger .

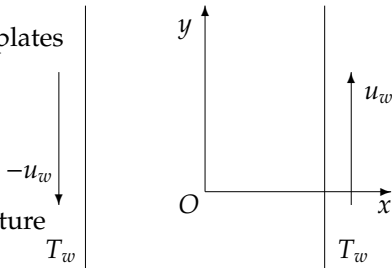
[†] V. E. Ambrus, V. Sofonea, Phys. Rev. E **89** (2014) 041301(R).

* G.P. Ghiroldi, L. Gibelli, Journal of Computational Physics **258** (2014) 568.

[‡] V. E. Ambrus, V. Sofonea, J. Comput. Phys., accepted.

Couette flow

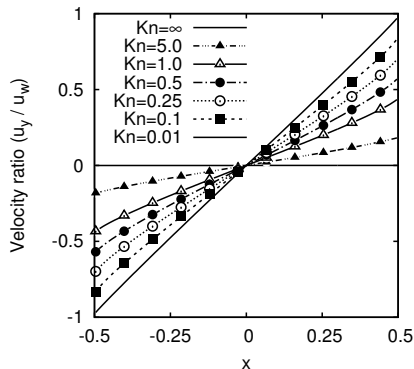
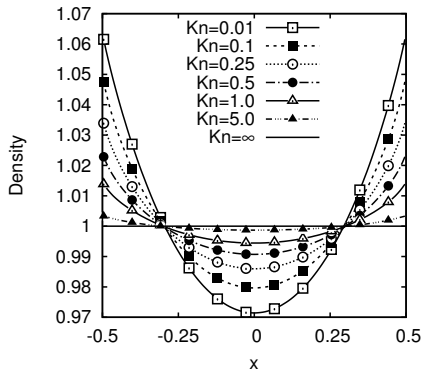
- 2D Couette flow between parallel plates ($x_+ = -x_- = -0.5$) moving along the y axis.
- Diffuse reflection on the x axis.
- $u_w = 0.63$, $T_w = 1.0$.
- Half-range models required to capture the discontinuous character of f .
- The reference profiles were obtained using the HHLB(21) \times HLB(4) model.



V. E. Ambruş, V. Sofonea, Phys. Rev. E **89** (2014) 041301(R) [3D, Shakhov]

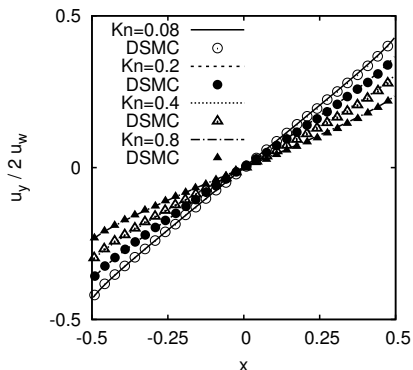
V. E. Ambruş, V. Sofonea, J. Comput. Phys., accepted

Reference profiles: n and u_y

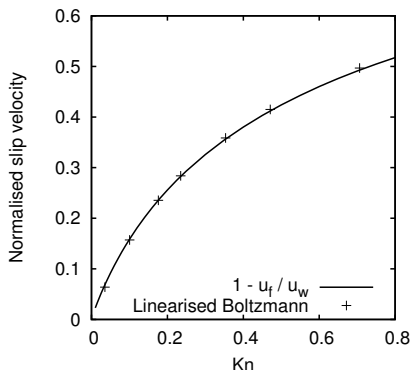


- $N = \int_{-L/2}^{L/2} dx n(x)$ fixed at unity for all Kn .
- $n(x_w)$ and $|u_w|$ decrease monotonically with Kn .

Comparison with DSMC & linearised Boltzmann



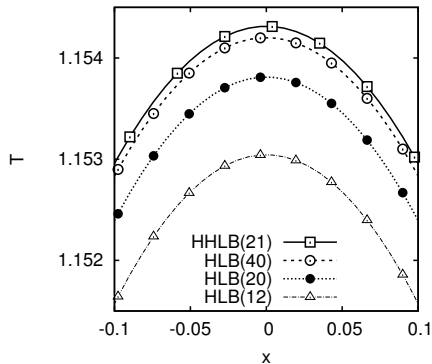
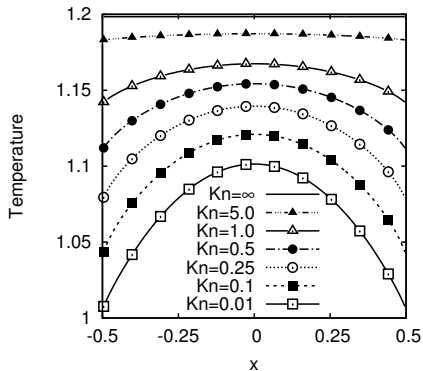
DSMC results from [†]



Linearised Boltzmann results from [†]

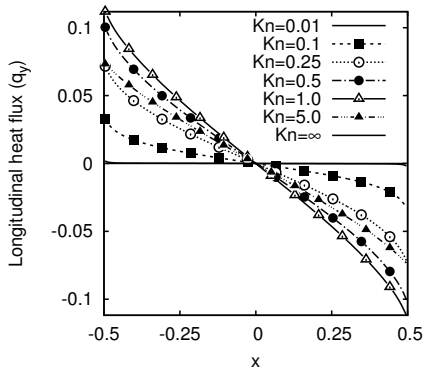
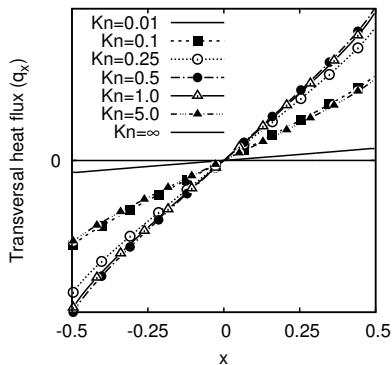
[†]S. H. Kim, H. Pitsch, I. D. Boyd, J. Comput. Phys. 227 (2008) 8655.

Reference profiles: T



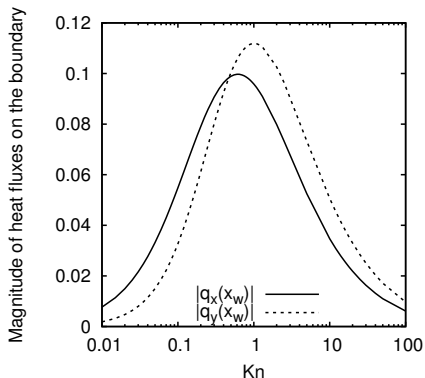
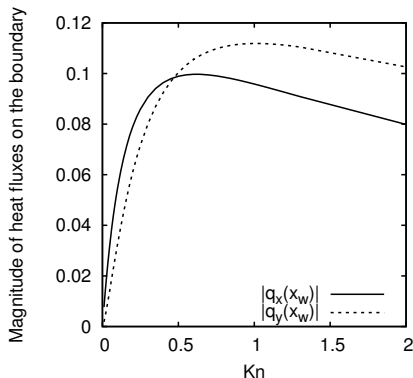
- T increases monotonically with Kn everywhere across the channel.
- $T^{\text{ballistic}} = T_w + mu_w^2/D$.

Reference profiles: q_x and q_y



- At small Kn , $f \sim f^{(eq)}$ (according to C-E), so q_x and q_y vanish.
- $q_x^{ballistic} = q_y^{ballistic} = 0$.

Dependence of $q_x(x_w)$ and $q_y(x_w)$ on Kn



- Maximum of $|q_x(x_w)|$ and $|q_y(x_w)|$ at $Kn \approx 0.62$ and 1.0 .

Y. Sone, *Molecular Gas Dynamics: Theory, Techniques and Applications*, Birkhäuser, Boston, 2007

Convergence test

- The following error is calculated for each profile $M \in \{n, u_y, T, q_x, q_y\}$:

$$\varepsilon_M = \frac{\max_x [M(x) - M_{\text{ref}}(x)]}{\Delta M_{\text{ref}}},$$

where $M_{\text{ref}}(x)$ represents the reference profile and

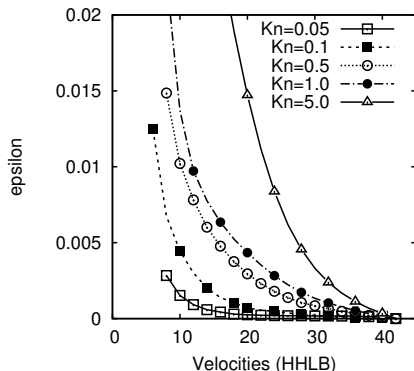
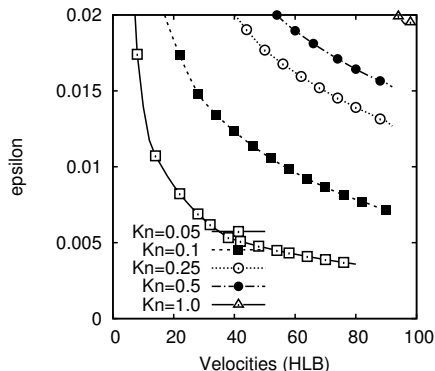
$$\Delta M_{\text{ref}} = \max\{\max_x [M_{\text{ref}}(x)] - \min_x [M_{\text{ref}}(x)], 0.1\}$$

- The restriction that $\Delta M_{\text{ref}} \geq 0.1$ is imposed to limit the effects of numerical fluctuations for quasi-constant profiles.
- Convergence is achieved in the channel domain when

$$\varepsilon \equiv \max_M (\varepsilon_M) \leq 0.01.$$

Full- vs half-range Hermite lattice Boltzmann models

2D Couette-BGK ($u_w = 0.63$)



- The HLB models do not converge for all $Q \leq 100$ for $Kn \gtrsim 0.25$.
- The HHLB models exhibit good convergence for all tested values of Kn .

V. E. Ambrus, V. Sofonea, J. Comput. Phys., accepted.

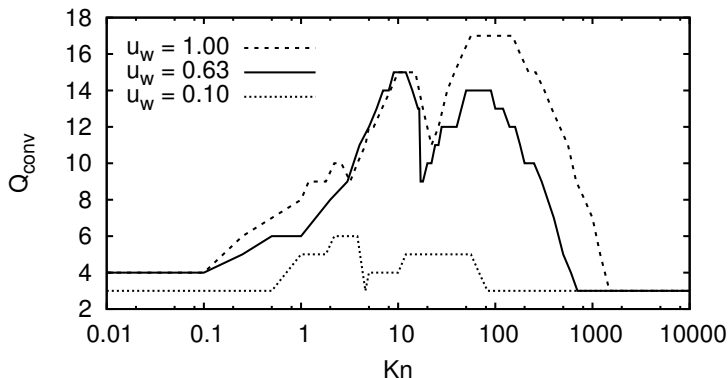
Convergence models

Kn	Number of velocities		
	$u_w = 0.1$	$u_w = 0.63$	$u_w = 1.0$
0.0005	18	32	32
0.001	18	32	32
0.01	18	32	32
0.05	18	32	32
0.1	18	32	32
0.25	18	40	48
0.5	18	48	56
1.0	40	48	64
5.0	32	96	96

The above data is for the models $\text{HHLB}(Q_x) \times \text{HLB}(Q_y)$, where $Q_y = \min(Q_x, 4)$. The number of velocities employed by such models is $2Q_x Q_y$.

V. E. Ambruş, V. Sofonea, J. Comput. Phys., accepted.

Convergence of HHLB over all Kn

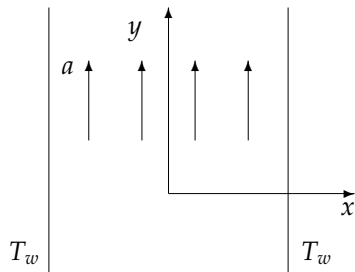


99% accuracy can be achieved throughout the whole spectrum of Kn using HHLB(6) \times HLB(4) ($2 \times 6 \times 4 = 48$ velocities) and HHLB(17) \times HLB(4) ($2 \times 17 \times 4 = 136$ velocities) for $u_w = 0.1$ and $u_w = 1.0$, respectively.

V. E. Ambrus, V. Sofonea, J. Comput. Phys., accepted.

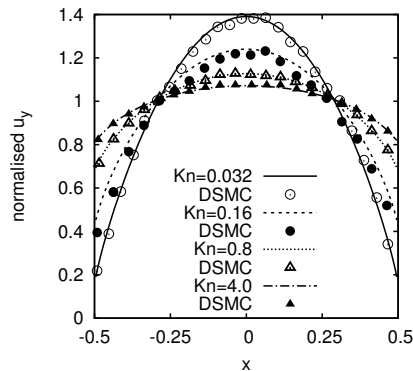
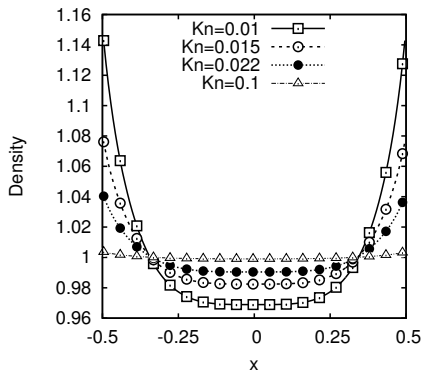
Poiseuille flow

- 2D Poiseuille flow between parallel plates at rest ($x_+ = -x_- = -0.5$).
- Diffuse reflection on the x axis.
- $a = 0.1$, $T_w = 1.0$.
- Half-range models required to capture the discontinuous character of f .
- The reference profiles were obtained using the HHLB(21) \times HLB(4) model.



V. E. Ambrus, V. Sofonea, *Journal of Computational Science*, under review.

Reference profiles: n and u_y

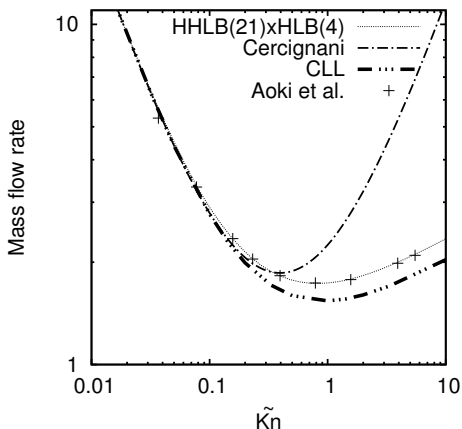


- $N = \int_{-L/2}^{L/2} dx n(x)$ fixed at unity for all Kn.
- $n(x_w)$ decreases monotonically with Kn.
- The agreement with DSMC[†] is excellent for u_y even at Kn = 4.0.

[†]S. H. Kim, H. Pitsch, I. D. Boyd, J. Comput. Phys. **227** (2008) 8655

Mass flow rate and velocity slip

2D Poiseuille-BGK ($a_y = 0.01$)

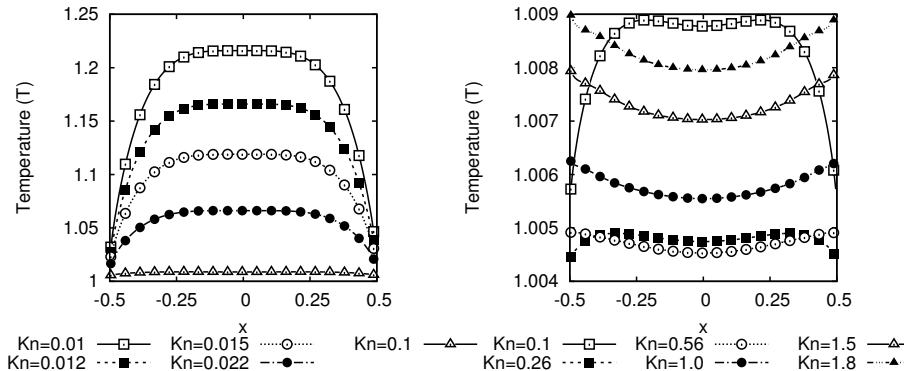


The mass flow rate is in excellent agreement with analytical predictions (at small Kn) and with the numerical DVM results of Aoki et al.[†].

[†] K. Aoki, S. Takata, T. Nakanishi, *Phys. Rev. E* **65** (2002) 026315.

Reference profiles: T

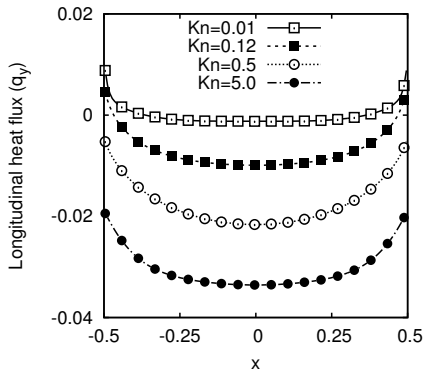
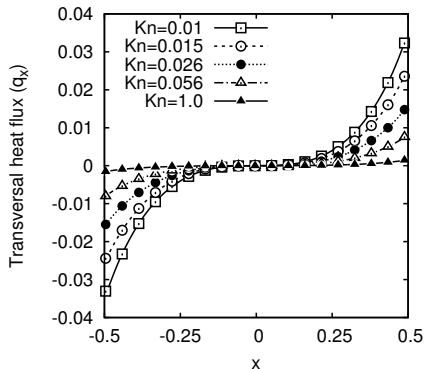
2D Poiseuille-BGK ($a_y = 0.1$)



T decreases monotonically with Kn , maintaining the shape of an inverted parabola for $Kn \lesssim 0.1$. For $Kn \gtrsim 0.1$, the profile becomes parabolic and the temperature increases monotonically with Kn .

Reference profiles: q_x and q_y

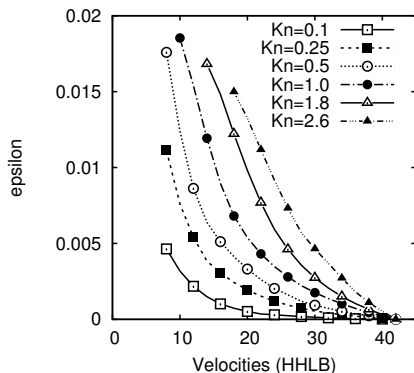
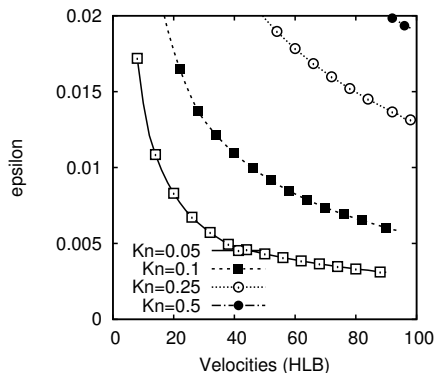
2D Poiseuille-BGK ($a_y = 0.1$)



- q_x decreases monotonically to 0 as $Kn \rightarrow \infty$.
- q_y decreases monotonically to $-\infty$ as $Kn \rightarrow \infty$.

Full- vs half-range Hermite lattice Boltzmann models

2D Poiseuille-BGK ($a_y = 0.1$)



- The HLB models do not converge for all $Q \leq 100$ for $Kn \gtrsim 0.25$.
- The HHLB models exhibit good convergence for $Kn \lesssim 2.6$.

V. E. Ambrus, V. Sofonea, *Journal of Computational Science*, under review.

Convergence models (Poiseuille flow)

Kn	Number of velocities		
	$a_y = 0.01$	$a_y = 0.05$	$a_y = 0.1$
0.01	32	32	32
0.05	18	32	32
0.1	18	18	32
0.25	18	18	40
0.5	18	32	48
1.0	18	40	64
5.0	40	96	136

The above data is for the models $\text{HHLB}(Q_x) \times \text{HLB}(Q_y)$, where $Q_y = \min(Q_x, 4)$. The number of velocities employed by such models is $2Q_x Q_y$.

V. E. Ambruş, V. Sofonea, *Journal of Computational Science*, under review.

Conclusion

- Quadrature-based LB models can be used to simulate thermal flows beyond the Navier-Stokes regime.
- Half-space quadratures are necessary in flows between diffuse reflective boundaries at non-negligible Kn.
- HLB (full-range) requires less velocities than HHLB (half-range) at small Kn, but converges very slowly when $\text{Kn} \approx 0.25$.
- The agreement in Poiseuille flow between LB and other numerical methods is excellent even at $\text{Kn} \sim 4.0$.
- This work was supported by a grant of the Romanian National Authority for Scientific Research, CNCS-UEFISCDI, project number PN-II-ID-JRP-2011-2-0060.